

Supplementary Information

Preparing Non-volatile Resistive Switching Memories by Tuning the content of Au@air@TiO₂-*h* Yolk-shell Microspheres in Poly(3-hexylthiophene) Layer

Peng Wang, Quan Liu, Chun-Yu Zhang, Jun Jiang, Li-Hua Wang, Dong-Yun Chen,
Qing-Feng Xu^a, Jian-Mei Lu^a

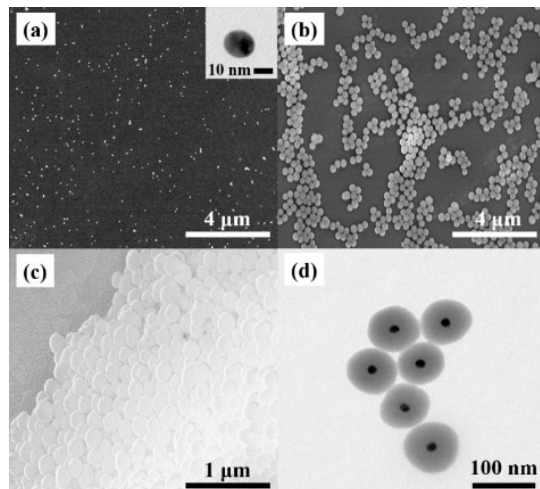


Figure S1. TEM and FESEM images of the (a) 16 nm Au nanocores, (b) (c) (d) 67 nm Au@SiO₂ microspheres. The respective scale bars for (a-d) are 4μm, 4μm, 1μm and 1μm. The insert showed the Au NPs at a scale about 10 nm

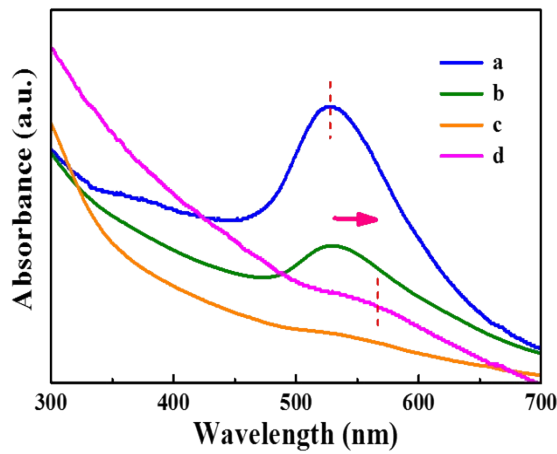


Figure S2. UV/Vis absorption spectra of (a) Au nanocores, (b) Au@SiO₂ microspheres, (c) Au@SiO₂@TiO₂-*h* microspheres, (d) Au@air@TiO₂-*h* yolk-shell microspheres dispersed in ethanol.

The UV/Vis absorption spectra of the Au nanocores, the Au@SiO₂ and Au@air@TiO₂-*h* yolk-shell hybrid microspheres dispersed in ethanol are shown in Fig. S2. The absorption peak of the Au@air@TiO₂-*h* nanospheres is red shifted from 525 nm to 560 nm and lower intensity compared to the Au NPs. And the red shift is due to an increase in the local refractive index of the medium surrounding the Au NPs¹.

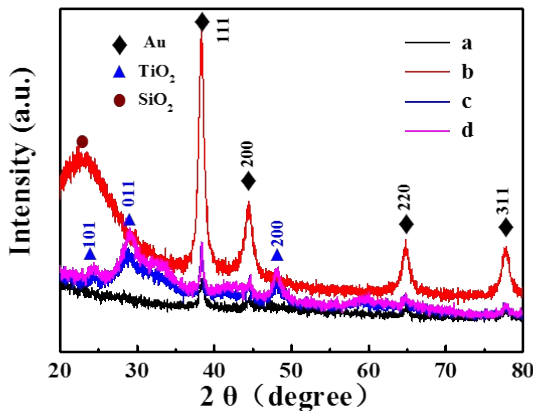


Figure S3. XRD patterns of the (a) Au nanocores, (b) Au@SiO₂ microspheres, (c) Au@SiO₂@TiO₂-*h* microspheres, (d) Au@air@TiO₂-*h* yolk-shell microspheres.

The crystal structures of the nanoparticles in different stages are further discerned by X-ray diffraction (XRD) patterns (Fig. S3). There are three series of peaks, which are respectively attributed to face-centered cubic Au (black rhombics), anatase-type TiO₂ (blue triangles) and amorphous-type SiO₂ (brown dots). Only peaks of Au and TiO₂ can be found in core-shell hollow spheres, indicating the yolk-shell nanoparticals have been successful synthesized.

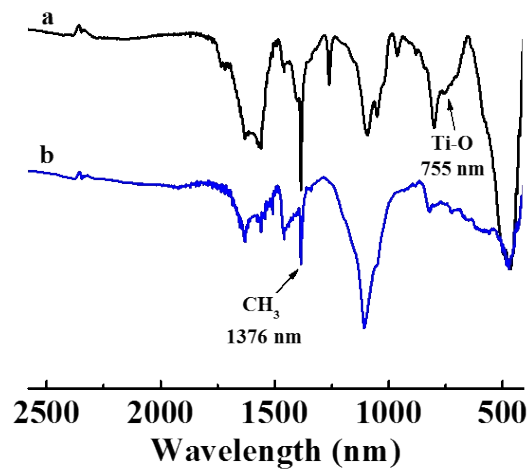


Figure S4. FT-IR absorption spectra of the (a) Au@air@TiO₂-h + P3HT, and (b) pure P3HT.

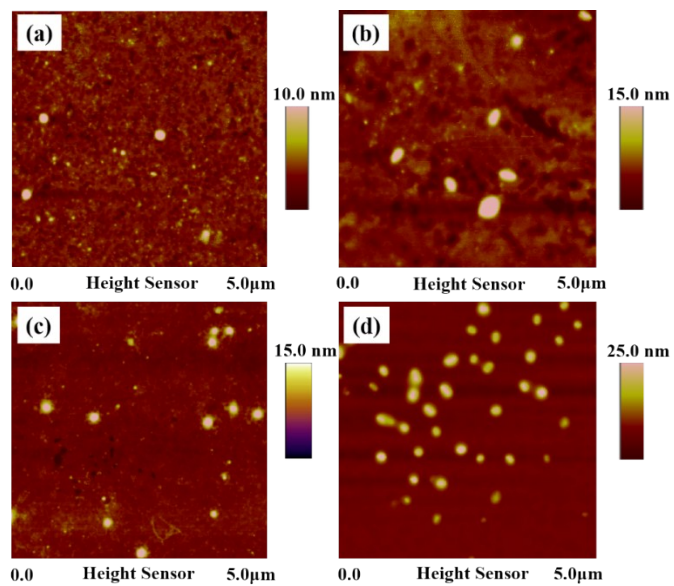


Figure S5. AFM 2D height images of the Au@air@TiO₂-*h* + P3HT polymer films containing: (a) 5 wt%, (b) 12 wt%, (c) 20 wt%, (d) 30 wt% Au@air@TiO₂-*h* microspheres for the switching device. The surface average roughness is 1.59 nm, 2.92nm, 1.28 nm, 9.96 nm, respectively.

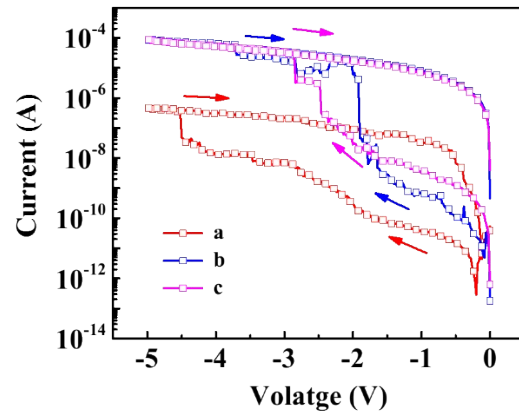


Figure S6. Typical current-voltage (*I*-*V*) characteristics of the (a) Al/[20 wt% Au NPs + P3HT]/ITO; (b) Al/[20 wt% Au@SiO₂ + P3HT] /ITO; (c) Al/[20 wt% Au@SiO₂@TiO₂-*h* + P3HT] /ITO switching device. ($I_{cc} = 10$ mA).

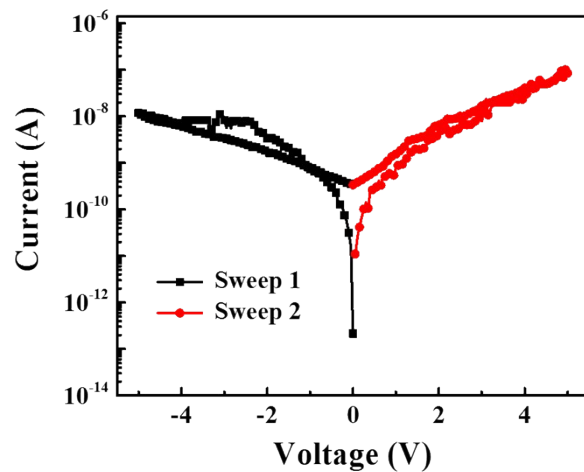


Figure S7. Typical current-voltage (*I*-*V*) characteristics of the Al/P3HT/ITO switching device. ($I_{cc}=10$ mA)

Reference

1. T. Cai, B. Zhang, Y. Chen, C. Wang, C.-X. Zhu, K.-G. Neoh and E.-T. Kang, *Chemistry – A European Journal*, 2014, **20**, 2723-2731.